

Differential directed flow in Au+Au collisions

A. Andronic^{4,1}, W. Reisdorf⁴, J.P. Alard³, V. Barret³, Z. Basrak¹², N. Bastid³, A. Bendarag³, G. Berek², R. Čaplar¹², P. Crochet³, A. Devismes⁴, P. Dupieux³, M. Dželalija¹², C. Finck⁴, Z. Fodor², A. Gobbi⁴, Yu. Grishkin⁷, O.N. Hartmann⁴, N. Herrmann⁶, K.D. Hildenbrand⁴, B. Hong⁹, J. Kecskemeti², Y.J. Kim⁹, M. Kirejczyk¹¹, P. Koczon⁴, M. Korolija¹², R. Kotte⁵, T. Kress⁴, R. Kutsche⁴, A. Lebedev⁷, Y. Leifels⁴, W. Neubert⁵, D. Pelte⁶, M. Petrovici¹, F. Rami¹⁰, B. de Schauenburg¹⁰, D. Schüll⁴, Z. Seres², B. Sikora¹¹, K.S. Sim⁹, V. Simion¹, K. Siwek-Wilczyńska¹¹, V. Smolyankin⁷, M.R. Stockmeier⁶, G. Stoicea¹, P. Wagner¹⁰, K. Wiśniewski⁴, D. Wohlfarth⁵, I. Yushmanov⁸, A. Zhilin⁷
(FOPI Collaboration)

¹ National Institute for Physics and Nuclear Engineering, Bucharest, Romania

² KFKI Research Institute for Particle and Nuclear Physics, Budapest, Hungary

³ Laboratoire de Physique Corpusculaire, IN2P3/CNRS, and Université Blaise Pascal, Clermont-Ferrand, France

⁴ Gesellschaft für Schwerionenforschung, Darmstadt, Germany

⁵ Forschungszentrum Rossendorf, Dresden, Germany

⁶ Physikalisches Institut der Universität Heidelberg, Heidelberg, Germany

⁷ Institute for Theoretical and Experimental Physics, Moscow, Russia

⁸ Kurchatov Institute, Moscow, Russia

⁹ Korea University, Seoul, South Korea

¹⁰ Institut de Recherches Subatomiques, IN2P3-CNRS, Université Louis Pasteur, Strasbourg, France

¹¹ Institute of Experimental Physics, Warsaw University, Poland

¹² Rudjer Boskovic Institute, Zagreb, Croatia

We present experimental data on directed flow in semi-central Au+Au collisions at incident energies from 90 to 400-A MeV. For the first time for this energy domain, the data are presented in a transverse momentum differential way. We study the first order Fourier coefficient v_1 for different particle species and establish a gradual change of its patterns as a function of incident energy and for different regions in rapidity.

PACS: 25.70.Lm, 21.65.+f, 25.75.Ld

The main motivation for the study of relativistic heavy ion collisions is to learn about the equation of state (EoS) of nuclear matter [1]. The collective phenomena [2] (see ref. [3,4] for recent reviews) were proposed as probes that preserve information about the transient hot and compressed state created in such collisions. The (in-plane) directed flow (also called sideways flow or transverse flow) was much studied, both experimentally [5–12] and theoretically [13–21]. The dependences of this phenomenon on incident energy, particle type and centrality have been determined experimentally (see ref. [3,4] and references therein), particularly for the Au+Au system. The balance energy, E_{bal} , which is the energy of “disappearance of flow”, was recently directly measured for Au+Au collisions [12]. It was found to be around 40-A MeV, somewhat lower than previous extrapolations [6,8,9]. The main features of the directed flow have been reproduced by the theoretical models, but a final conclusion on the EoS has not yet been achieved. As pointed out early on [13–15], the momentum dependent interactions (MDI) play a crucial role in the determination of the EoS. Together with the (in-medium) nucleon-nucleon cross section (σ_{nn}), MDI has a marked influence on the

directed flow [18,19,21]. Moreover, consistency is needed in deriving EoS together with both MDI and σ_{nn} [17].

All the above-mentioned results have been obtained in a transverse momentum (p_t) integrated way, usually by studying the average in-plane transverse momentum, $\langle p_x \rangle$, as a function of rapidity, y . The analysis of flow in terms of p_t dependence of the first order Fourier coefficient, which we shall call “differential directed flow” (DDF), has been proposed by Pan and Danielewicz [18], who found it sensitive to MDI. Li and Sustich have studied the sensitivity of DDF to both EoS and nucleon-nucleon cross section (σ_{nn}) around the balance energy [21]. They found complex patterns of DDF, a vanishing slope of the $\langle p_x \rangle - y$ distribution being the result of averaging over transverse momenta. The DDF was extensively exploited at AGS energies both experimentally, by the E877 collaboration [22], and theoretically [23]. It was found to be sensitive to the characteristics of the transverse expansion and on the EoS, especially at high p_t [23]. For our energy domain, apart from its importance in revealing the dynamics of the heavy ion collisions, the differential flow could ultimately help towards pinning down the stiffness of the EoS of hot and dense nuclear matter formed in such collisions [18,24].

In this Rapid Communication we present experimental data on directed flow for Au+Au collisions at incident energies of 90, 120, 150, 250 and 400-A MeV. Along with the integrated distributions, the data are presented in a p_t differential way for the first time for this energy domain. The DDF is analyzed for different particle species and as a function of rapidity.

The data have been measured with a wide phase-space coverage using the FOPI detector [25] at GSI Darmstadt. The reaction products were identified by charge (Z) in the

forward Plastic Wall (PW) at $1.2^\circ < \Theta_{lab} < 30^\circ$ using time-of-flight and specific energy loss. In the Central Drift Chamber (CDC), covering $34^\circ < \theta_{lab} < 145^\circ$, the particle identification is obtained using magnetic rigidity and the energy loss. For more details on the detector configuration for this experiment see ref. [26].

For the centrality selection we used the charged particles multiplicities, classified into five bins. The variable $E_{rat} = \sum_i E_{\perp,i} / \sum_i E_{\parallel,i}$ (the sums run over the transverse and longitudinal c.m. kinetic energy components of all the products detected in an event) has been additionally used for a better selection of the most central collisions. The geometric impact parameters interval for our centrality region M4, for which the results are presented here, is 2.0–5.3 fm. We note that in this bin the directed flow exhibits a maximum as a function of centrality [3,11].

To compare different incident energies, we use normalized center-of-mass (c.m.) transverse momentum (per nucleon) and rapidity, defined as:

$$p_t^{(0)} = (p_t/A)/(p_P^{cm}/A_P), \quad y^{(0)} = (y/y_P)^{cm} \quad (1)$$

where the subscript P denotes the projectile.

The reaction plane has been reconstructed event-by-event using the transverse momentum method [27]. All particles in an event have been used for the reaction plane reconstruction, excluding the particle-of-interest to prevent autocorrelations and a window around midrapidity ($|y^{(0)}| < 0.3$) to improve the resolution. The correction of the extracted values due to the reconstructed reaction plane fluctuations has been done using the recipe of Ollitrault [28]. The correction factors, $1/\langle \cos \Delta\phi \rangle$, where $\Delta\phi$ is the resolution of the reaction plane azimuth, are presented in Table I for the five incident energies, along with the projectile momenta per nucleon in the c.m. system, p_P^{cm}/A_P .

TABLE I. Projectile momentum (per nucleon) in the center of mass and the correction factor for the reaction plane resolution.

| E (A MeV) | 90 | 120 | 150 | 250 | 400 |
|-------------------------------------|------|------|------|------|------|
| p_P^{cm}/A_P (MeV/c) | 205 | 237 | 265 | 342 | 433 |
| $1/\langle \cos \Delta\phi \rangle$ | 1.51 | 1.18 | 1.10 | 1.05 | 1.04 |

An important ingredient in the present analysis is the correction for distortions due to multiple hit losses. As an example, in case of PW, despite its good granularity (512 independent modules [25]), average multiple hit probabilities of up to about 9% at 400-A MeV are registered for the multiplicity bin M4. Because of the directed flow, the average number of particles detected over the full PW subdetector is 2 times higher than out of the reaction plane. This leads to an underestimation of the directed flow and needs to be taken into account. We developed a correction procedure based on the experimental data, by exploiting the DDF left-right symmetry with respect

to midrapidity. The correction depends on $p_t^{(0)}$ and incident energy. It reaches 12% for the energy of 400-A MeV and is almost negligible at 90-A MeV. The procedure was checked and validated using IQMD (Isospin Quantum Molecular Dynamics [16]) events passed through a full GEANT simulation of the detector.

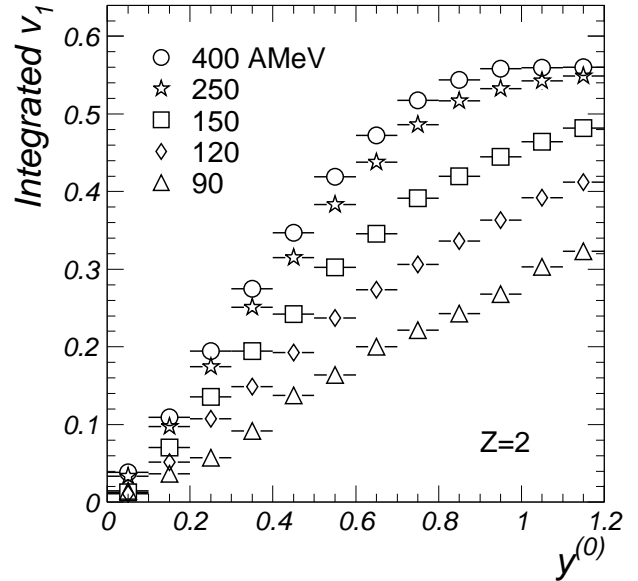


FIG. 1. Integrated v_1 values as a function of rapidity for five incident energies, M4 centrality bin, for $Z=2$ particles.

We characterize the directed flow by the first order Fourier coefficient: $v_1 = \langle \cos(\phi) \rangle$ where ϕ is the angle with respect to the reaction plane. In Fig. 1 we present for $Z=2$ particles the values of the v_1 coefficient integrated over transverse momentum. These distributions are for the forward hemisphere and were obtained by combining the information of both PW and CDC. Note that, for the phase space coverage of CDC, $Z=2$ sample comprises only alpha particles. We mention that the slopes at midrapidity of the equivalent $\langle p_x \rangle - y^{(0)}$ distributions are in perfect agreement with the FOPI results from Phase I data [9].

Two important features can be emphasized from the distributions presented in Fig. 1. First, we are in a region where the flow is strongly increasing as a function of incident energy [9], as a result of stronger compression. This is contrary to expectations based on ideal hydrodynamics [29] and has been related to a possible liquid-gas phase transition which breaks the scaling behaviour [29,9]. Second, the shape as a function of rapidity is evolving with the incident energy. For higher energies, a saturation of the v_1 coefficient is seen for the projectile rapidities. Weighted with the (rapidity dependent) transverse momentum spectra it leads to the well known so-called “S curve” in the $\langle p_x \rangle - y$ distributions [5,7–9,11] which was interpreted as a result of “bounce-off” from the spectators. At lower energies, the steady evolution of v_1 as a function of y points to a poorer separation of the participant and spectator contributions, probably as a result

of a relatively stronger Fermi motion. Intuitively, longer passing times might as well allow for larger cross-talk and “equilibration” between participant and spectators.

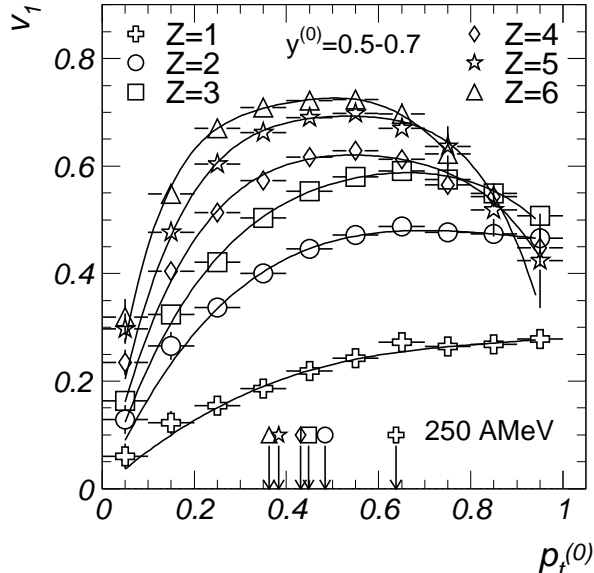


FIG. 2. The dependence of the v_1 coefficient on transverse momentum for 250-A MeV incident energy, M4 centrality bin, for different particles. The lines are polynomial fits to guide the eye. The arrows mark the values of the average $p_t^{(0)}$ for each particle.

In Fig. 2 we show the differential flow for particles with charge $Z=1$ to $Z=6$ for the incident energy $E=250$ -A MeV. We selected the rapidity window $0.5 < y^{(0)} < 0.7$, corresponding to the maximum of the directed flow in the $\langle p_x \rangle$ - y representation. From here on, to keep a clean particle selection on Z , we limit our p_t domain to the PW acceptance (which translates in a rapidity-dependent upper $p_t^{(0)}$ limit). The error bars on v_1 include both statistical and systematical errors, the latter coming from the apparatus acceptance. The horizontal bars indicate the $p_t^{(0)}$ bin width. The arrows, labeled by the corresponding symbols, are indicating the average values of $p_t^{(0)}$ for the fragments analyzed. The lines here and in the following figures are polynomial fits to guide the eye. For the chosen rapidity window the multiplicities of the fragments up to $Z=6$ relative to $Z=1$ are in the ratios 1000/380/68/20/14/8. We first remark that the flow of heavier fragments is larger, a fact established in an integrated way by many experiments [8,11] and interpreted as a signature of a collective phenomenon [28]. As was demonstrated in ref. [11], this is the result of the interplay of the thermal and collective motion. For the lighter particles the thermal contribution is higher relative to the collective one, leading to a lower “apparent” flow. One can see in Fig. 2 that not only the magnitude is increasing, but also that the pattern of v_1 changes for heavier particles, for which a maximum develops at steadily lower scaled momenta. The increase of the anisotropy as a function of p_t is very rapid and compatible with a linear

one only in a very narrow p_t region. Note that at AGS energies a linear dependence of v_1 on p_t was established experimentally for different particle species over a broad p_t interval [22].

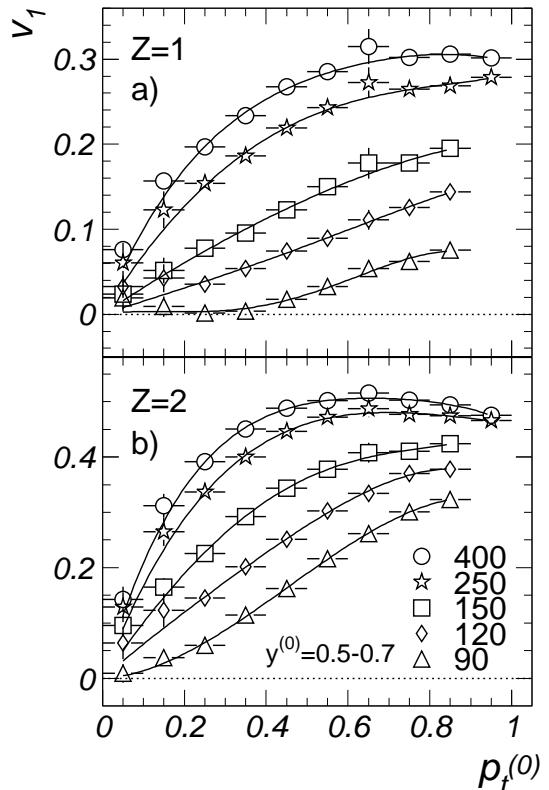


FIG. 3. The dependence of the v_1 coefficient on transverse momentum for five incident energies, M4 centrality bin, for $Z=1$ and $Z=2$ particles.

Fig. 3 presents, for our five incident energies, the dependence of the v_1 coefficient on the normalized transverse momentum for $Z=1$ and $Z=2$ particles in the rapidity window $0.5 < y^{(0)} < 0.7$. The two particle species show different patterns of DDF as function of incident energy. For the lowest incident energy, 90-A MeV, while for $Z=1$ particles the flow is close to zero for the low $p_t^{(0)}$ part and shows a later onset, in the case of $Z=2$ fragments one can notice a steady increase of v_1 as a function of $p_t^{(0)}$. Although with smaller magnitude (as we are well above E_{bal}), the $Z=1$ case is similar to the behavior predicted by Li and Sustich at E_{bal} [21]. The coexistence of two flow patterns, attractive and repulsive, was explained in ref. [21] by the fact that the low p_t particles suffer more the influence of the attractive mean field, leading to a negative v_1 , while at high p_t the repulsive nucleon-nucleon scatterings are responsible for the positive flow. The particular feature of DDF seen at 90-A MeV is rapidly changing as a function of incident energy, the increase of v_1 as a function of p_t becoming gradually steeper for higher energies.

For both particle species there is a gradual development of a limiting value of DDF at high $p_t^{(0)}$ as the in-

cident energy increases. Part of these high- p_t particles could have been emitted at a pre-equilibrium stage, therefore not reaching the maximum compression stage of the reaction. For the corresponding rapidity window, the average transverse momentum of $Z=1$ particles has a more pronounced variation compared to $Z=2$ (see Table II), presumably as a result of a different participation of different particle types in the reaction dynamics at these energies [30]. Also, $Z=2$ particles can originate to a large extent from secondary decays of heavier fragments [19]. It would be important to study these details using transport models.

TABLE II. Average normalized transverse momentum for particles with $Z=1$ and $Z=2$ for the rapidity window $y^{(0)}=0.5-0.7$.

| Energy (A MeV) | 90 | 120 | 150 | 250 | 400 |
|---------------------------------|------|------|------|------|------|
| $\langle p_t^{(0)} \rangle$ Z=1 | 0.74 | 0.71 | 0.67 | 0.63 | 0.60 |
| $\langle p_t^{(0)} \rangle$ Z=2 | 0.51 | 0.50 | 0.49 | 0.48 | 0.48 |

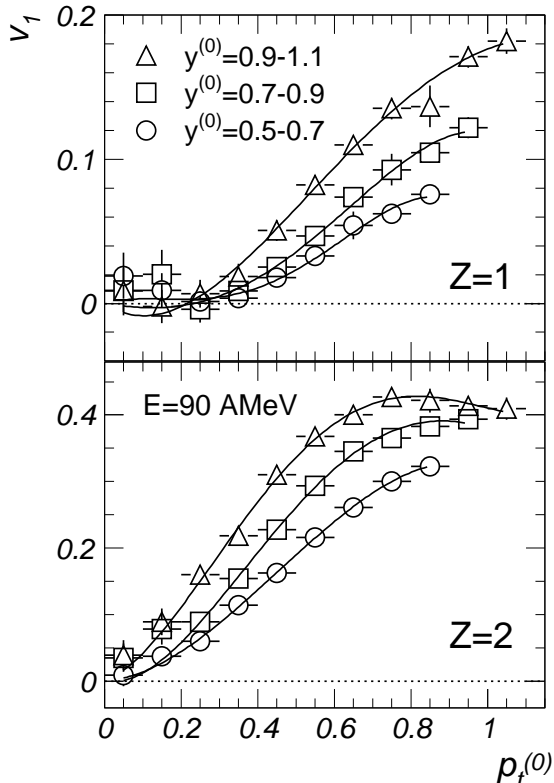


FIG. 4. v_1 as a function of transverse momentum in three windows in rapidity for particles with $Z=1$ and $Z=2$ for the incident energy of 90-A MeV.

From our differential flow values at 90-A MeV one can infer that E_{bal} is not a single-defined value but is dependent on particle type and on transverse momentum. We have observed similar trends in what concerns E_{tran} , the energy of the transition from in-plane to out-of-plane azimuthal enhancement at midrapidity [26]. As E_{bal} is

decreasing as a function of p_t , its integrated value cannot be compared among various experiments unless their different thresholds are taken into account. Moreover, E_{bal} can depend on rapidity as well, as shown in Fig. 4, where the DDF is presented for $Z=1$ and $Z=2$ particles for three windows in rapidity for the incident energy of 90-A MeV. Notice again the difference between the two particle species in what concerns the patterns of the flow and that at projectile rapidities (triangles) the anisotropy of $Z=2$ particles already develops a maximum, in contrast to $Z=1$ particles.

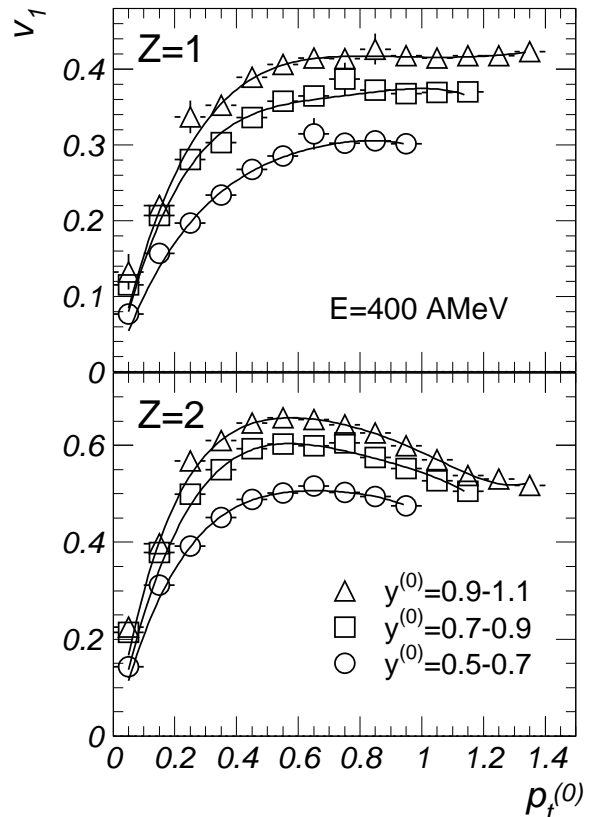


FIG. 5. Same as Fig. 4, but for the incident energy of 400-A MeV.

While at our lowest incident energy of 90-A MeV the DDF may help towards pinning down the in-medium nucleon-nucleon cross section [21], at higher energies it may bear significance on the MDI [18] and ultimately on the EoS. The rapidity dependence of the DDF at the incident energy of 400-A MeV is presented in Fig. 5 for $Z=1$ and $Z=2$ particles. Again, at all rapidities there is a clear difference in shape between the two particle species. For $Z=2$ particles notice that at projectile rapidities ($y^{(0)}=1$) the anisotropy is highest (see also Fig. 1), while the $\langle p_x \rangle$ values would already show a decreasing trend [5,7-9,11].

For both incident energies, Fig. 4 and 5, one can see that the shape of the distributions varies as a function of rapidity, giving additional support for the influence of the dynamics of the collision on the flow values. Also, the maximum of v_1 for $Z=2$ (for $y^{(0)}=0.9-1.1$) for the energy of 400-A MeV occurs at a different value of transverse

momentum compared to 90-A MeV, either in terms of scaled or not scaled momenta.

In summary, we have shown first experimental results on differential directed flow in heavy ion collisions at incident energies from 90 to 400-A MeV. Our p_t differential study allows us to show that not only is the flow larger, but also its pattern is different for heavier particles. In addition, it has a complex evolution as a function of beam energy. The differential flow pattern of $Z=1$ and $Z=2$ particles was studied as well for different regions in rapidity.

It is expected that the DDF will help to clear the difficulties (and sometimes inconsistencies) noticed in previous studies devoted to directed flow using comparisons with transport models, either of QMD-type [13,16,17,8,10] or from the Boltzmann-Uehling-Uhlenbeck (BUU) family [14,18,20]. Present comparisons of the experimental differential directed flow to BUU [31] or IQMD [32] models show sensitivities to the EoS. But, if the EoS is to be extracted from such types of comparisons, more effort is needed, especially in disentangling the contributions of momentum dependent interactions and in-medium nucleon-nucleon cross sections from the EoS itself. It is in the energy range of the present study that both MDI and σ_{nn} have a very important contribution and cannot at all be neglected. Along with the centrality dependence of directed flow [13,18,10] and with the differential elliptic flow [24], the DDF can contribute to a good extent in fixing these quantities [18,21]. Properly incorporating the fragment production [19] and a consistent treatment of the momentum dependent interactions [17,19,20] and in-medium nucleon-nucleon cross sections are essential prerequisites for this task.

This work has been supported in part by the German BMBF under contracts RUM-005-95, POL-119-95, UNG-021-96 and RUS-676-98 and by the Deutsche Forschungsgemeinschaft (DFG) under projects 436 RUM-113/10/0, 436 RUS-113/143/2 and 446 KOR-113/76/0, Support has also been received from the Polish State Committee of Scientific Research, KBN, from the Hungarian OTKA under grant T029379, from the Korea Research Foundation under contract No. 1997-001-D00117, from the agreement between GSI and CEA/IN2P3 and from the PROCOPE Program of DAAD.

- [6] W.M. Zhang et al., Phys. Rev. C **42**, R491 (1990)
- [7] V. Ramillien et al., Nucl. Phys. A **587**, 802 (1995)
- [8] M.D. Partlan et al., Phys. Rev. Lett. **75**, 2100 (1995)
- [9] P. Crochet et al., Nucl. Phys. A **624**, 725 (1997)
- [10] P. Crochet et al., Nucl. Phys. A **627**, 522 (1997)
- [11] F. Rami et al., Nucl. Phys. A **646**, 367 (1999)
- [12] D.J. Magestro et al., Phys. Rev. C **61**, 021602(R) (2000)
- [13] J. Aichelin, A. Rosenhauer, G. Peilert, H. Stöcker and W. Greiner, Phys. Rev. Lett. **58**, 1926 (1987)
- [14] C. Gale, G.M. Welke, M. Prakash, S.J. Lee and S. Das Gupta, Phys. Rev. C **41**, 1545 (1990)
- [15] B. Blättel, V. Koch, A. Lang, K. Weber, W. Cassing and U. Mosel, Phys. Rev. C **43**, 2728 (1991)
- [16] J. Aichelin, Phys. Rep. **202**, 233 (1991)
- [17] J. Jaenicke, J. Aichelin, H. Ohtsuka, R. Linden and A. Faessler, Nucl. Phys. A **536**, 201 (1992)
- [18] Q. Pan and P. Danielewicz, Phys. Rev. Lett. **70**, 2062 (1993)
- [19] A. Ono, H. Horiuchi and T. Maruyama, Phys. Rev. C **48**, 2946 (1993)
- [20] C. Fuchs, T. Gaitanos and H.H. Wolter, Phys. Lett. B **381**, 23 (1996)
- [21] B.-A. Li and A. Sustich, Phys. Rev. Lett. **82**, 5004 (1999)
- [22] J. Barette et al., Phys. Rev. C **59**, 884 (1999)
- [23] B.-A. Li, C.M. Ko and G.Q. Li, Phys. Rev. C **54**, 844 (1996)
- [24] P. Danielewicz, Nucl. Phys. A **673**, 375 (2000)
- [25] A. Gobbi, FOPI Collaboration, Nucl. Instr. and Meth. in Phys. Res. A **324**, 156 (1993); J. Ritman, Nucl. Phys. B (Proc. Suppl.) **44** (1995) 708.
- [26] A. Andronic et al., Nucl. Phys. A **679**, 765 (2001)
- [27] P. Danielewicz and G. Odyniec, Phys. Lett. B **157**, 146 (1985)
- [28] J.-Y. Ollitrault, nucl-ex/9711003, Nucl. Phys. A **638**, 195 (1998)
- [29] A. Bonasera and L.P. Csernai, Phys. Rev. Lett. **59**, 630 (1987)
- [30] M. Petrovici et al., Phys. Rev. Lett. **74**, 2001 (1995); R. Kotte et al., Eur. J. Phys. A **6**, 185 (1999)
- [31] T. Gaitanos, C. Fuchs, H.H. Wolter and A. Faessler, arXiv:nucl-th/0102010
- [32] A. Andronic et al., in preparation

-
- [1] H. Stöcker and W. Greiner, Phys. Rep. **137**, 277 (1986)
 - [2] H. Stöcker, J.A. Maruhn and W. Greiner, Phys. Rev. Lett. **44**, 725 (1980)
 - [3] W. Reisdorf and H.G. Ritter, Ann. Rev. Nucl. Part. Sc. **47**, 663 (1997)
 - [4] N. Herrmann, J.P. Wessels and T. Wienold, Ann. Rev. Nucl. Part. Sc. **49**, 581 (1999)
 - [5] K.G.R. Doss et al., Phys. Rev. Lett. **57**, 302 (1986)